Manuscript version: 6 November 2019
Elsevier, Materials Science & Engineering
https://doi.org/10.1016/j.msea.2019.138639

Strength-ductility trade-off via SiC nanoparticle dispersion in A356 aluminium matrix

R. Taherzadeh Mousavian, S. Behnamfard, R. AzariKhosroshahi, J.Zavašnik, P.Ghosh S.Krishnamurthy, A. Heidarzadeh, D.Brabazon

[a]I-Form, Advanced Manufacturing Research Centre & Advanced Processing Technology Research Centre, School of Mechanical & Manufacturing Engineering, Dublin City University, Dublin 9, Ireland
[b]Faculty of Materials Engineering, Sahand University of Technology, Tabriz, Iran
[c]Jožef Stefan Institute, Jamova 39, 1000, Ljubljana, Slovenia
[d]Nanoscale Energy and Surface Engineering Department of Engineering and Innovation, The Open University, Buckinghamshire, MK7 6AA, United Kingdom
[e]Department of Materials Engineering, Azarbaijan Shahid Madani University, Tabriz, Iran

corresponding author. rezataherzadeh.mousavian@dcu.ie

Abstract

A process was developed to disperse β-SiC nanoparticles (NPs), with a high propensity to agglomerate, within a matrix of A356 aluminum alloy. A suitable dispersion of 1 wt% SiC NPs in the A356 matrix was obtained through a hybrid process including a solid-state modification on the surface of the NPs, a two-step stirring process in the semi-solid and then the liquid-state, and a final hot-rolling process for fragmentation of the brittle eutectic silicon phase and porosity elimination. Titanium and nickel where used as the nanoparticle SiC surface modifiers. Both modifiers were found to improve the mechanical properties of the resulting material, however, the highest improvement was found from the nickel surface modification. For the nickel modification, compared to the non-reinforced rolled alloy, more than a 77%, 85%, and 70% increase in ultimate tensile strength (UTS), yield strength (YS), and strain % at the break, respectively were found with respect to the unreinforced rolled A356. For the rolled nanocomposite containing 1 wt % SiC_{np} and nickel modification, an average YS, UTS, and strain % at the break of 277 MPa, 380 MPa, and 16.4% were obtained, respectively, which are unique and considerable property improvements for A356 alloy

Keywords, SiC NPs, Aluminium nanocomposite, Nanoparticles, Mechanical properties

To cite this article: *R. Taherzadeh Mousavian, S. Behnamfard, R. AzariKhosroshahi, J.Zavašnik, P.Ghosh S.Krishnamurthy, A. Heidarzadeh, D.Brabazon, Strength-ductility trade-off via SiC nanoparticle dispersion in A356 aluminium matrix, Materials Science & Engineering A 771 (2020) 138639*

Manuscript version: 6 November 2019
Elsevier, Materials Science & Engineering
https://doi.org/10.1016/j.msea.2019.138639

1. Introduction

The unabated thirst for fuel-saving and cost-efficient materials in automotive, defense, and aerospace industries has generated a focus on metal matrix nanocomposites (MMNCs). The primary goal of MMNC research is to employ nanoparticle (NP) reinforcements to produce high strength/low-density materials with a higher ductility than can be achieved by using micron-size reinforcements. In this case, a suitable dispersion of NPs can be used as a barrier for the movement of dislocations and avoid their pile up on grain boundaries [1]. However, the characteristic nature of the high surface-to-volume ratio and van der Waals forces between the NPs tend to keep them in the agglomerated state. Several different approaches have been examined (e.g. sonication, particle heat treatment, and various mixing methods) to break the bonds and thereby deagglomerate the clusters [2,3].

Two major routes for MMNCs processing have been developed, solid-state processing (e.g. powder metallurgy) and liquid-state solidification processing [4]. In the powder metallurgy route, high shear stress generated by high-energy ball milling is used to shear nanoparticle clusters. However, this technique contains various drawbacks. The cost of metal powder production is high, and this method has limited capability for shaping products in geometrically complex forms. Furthermore, this method needs additional processes to manufacture the final parts, such as HIP'ing, machining, or another surface finishing [5,6]. The casting method (liquid-state solidification processing) can be conducted in liquid, semi-solid, or in a two-step process, which has been used to overcome the noted drawbacks of the powder metallurgy route. This method is suitable to produce components with complex shapes in any sizes. Also, it is a low cost, convenient, and accessible technique. The Casting of an MMNC where Orowan strengthening is dominant requires dispersion of NPs in the liquid melt followed by the engulfment of the particles within the solidifying grains which is one of the most challenging methods for achieving a uniform NP dispersion. It is known that a uniform distribution of NPs inside the grains is difficult to achieve in practice to pin the dislocations. Whether particles are pushed or engulfed during solidification depends on the velocity of the particles relative to the solidification front (SF) during grain growth. If the SF velocity is higher than the critical velocity, the particles will be engulfed by the moving SF. Assuming the velocity of the SF is held constant, NPs in low concentrations can thereby be engulfed [1]. Therefore, to design the microstructure of MMNCs, the interaction of NPs with an advancing solid-liquid interface and methods for their injection to the melt need to be studied [7].

Various measurements have been taken to address the problems associated with NPs agglomeration, such as semi-solid stir casting (SS-SC) [[2], [3], [4]], ultrasonic treatment [[5], [6], [7], [8], [9], [10], [11], [12], [13]], ball-milling [[14], [15], [16]] as well as a combination of these routes [[17], [18], [19], [20]]. It has been reported that in the SS-SC process, shear stress in the two-phase region causes dis-agglomeration. Rohatgi [21] and his research team investigated the manufacture of aluminum-based nanocomposites by using a reactive wetting method in which magnesium chips were added to react with the alumina layer on the surface of aluminum alloy. They reported that magnesium, as it is introduced in the molten metal, could eliminate the oxygen and surface alumina by reacting with Al_2O_3. Indeed, Mg improves the wettability by removing surface alumina and decreasing surface tension or interfacial energy between particles and melt. They showed that in the case of achieving an ideal distribution of nanoparticles without any clustering, the grains remain coarse and Orowan is the dominant strengthening mechanism. If agglomeration takes place, the clusters are moved by the solidification front and accumulation of clusters leads to the production of smaller grains, and the dominant strengthening mechanism, in this case, is Hall-Petch.

The idea of using a carrier protein, which is a method used in medical science to inject specific substances into the blood was suggested by Su et al. [22]. In this study, it was showed that aluminum powder is a suitable carrier to introduce nanoparticles into the melt. However, no low-magnification microstructure was reported in their study for concluding the method of incorporation. In 2014 Rohatgi et al. [23] evaluated strengthening mechanisms with the addition of magnesium as the wetting factor to the melt. Nano-alumina powders were added to melt in two forms, once covered in foils without compression, and once compacted and pressed by foils. However, the agglomeration of NPs was shown in their results. Zhou et al. [24] used nickel coatings for nanoparticles before adding them into the melt to improve the wettability. However, sub-micron sized clusters were detected inside the grains. Also, it was not reported in their study that how they coated nano-sized ceramics with a nickel layer, which individually separately is not a trivial task. Two studies were conducted by Rohatgi et al. [1,25] regarding the Brownian motion of nanoparticle and the possibility of trapping these particles by the solidification front. They showed that the Brownian motion of nanoparticles or low rates of nanoparticles could be dominant, and there is a critical amount for nanoparticles to be added in composites. They illustrated that by the addition of nanoparticles in small volume fractions, they could be trapped and captured by solidification front due to Brownian motion, while larger submicron particles are more prone to be moved by solidification front and clustering. Zhang et al. [20] milled nano silicon carbide powders with Al2014 alloy powders to improve their wettability within the liquid alloy. They reported an improvement in strength, while provided microstructures which showed agglomeration of NPs in the metal matrix. A distinct study was reported [12], in which a liquid Mg–Zn matrix was reinforced by SiC nanoparticles. They dispersed 1%. vol NPs in the liquid matrix by using ultrasonic waves, and a high percentage of matrix alloy was vaporized via an assisting vacuum pump. They achieved a unique and ideal microstructure. It should be noted that this method is not suitable and applicable to all types of light metals, as the matrix should be evaporated to some extent. Vishwanatha et al. [13] tried to provide an approach that would eliminate the disadvantages of both contact and non-contact ultrasonic methods for the dispersion of nanoparticles. For this purpose, a contact-type ultrasonic method was used. Then the liquid mixture was transferred into another chamber with a bottom pouring system to enhance the distribution of nanoparticles using a non-contact ultrasonic method. They provided the microstructures from three methods of 1. Contact, 2.non-contact and 3. A combination of contact and non-contact types, which showed the inability of contact and non-contact ultrasonic methods for the distribution of nano-ceramic particles in their metal matrix. It also was observed that while a better dispersion was obtained with the combination method, an appropriate uniform distribution was not achieved in the produced nanocomposites. The contamination of the liquid melt because of contact between the probe tip and the liquid melt was reported to be a severe problem and for the non-contact ultrasonic treatment, the acoustic energy to the liquid melt is transmitted through the mould wall and the drawback of this method is that the processing time is typically too short to achieve complete deagglomeration. Also, the ultrasonic intensity is very limited on the surface of the melt, and it is a time-consuming process to introduce the nanoparticles into the melt using ultrasonic vibration.

To the best knowledge of authors, a uniform distribution of nanoparticles has not been accomplished in Al–Si alloys by the mentioned methods, and the reinforcements still have a relatively poor wettability and a high tendency to cluster propagated by the present Van-der-Waals forces.

Manuscript version: 6 November 2019
Elsevier, Materials Science & Engineering
https://doi.org/10.1016/j.msea.2019.138639

A356 is a hypoeutectic Al–Si alloy, consisting of plate-like eutectic silicon and α-aluminium primary phase dendrites. To improve the mechanical properties of these alloys, efforts have been made to develop aluminium matrix composites (AMCs) reinforced by ceramic particles. In Table 1, a summary of related reports for A356-based composites is tabulated. It can be observed that various methods and reinforcement have been applied to reinforce A356 alloy, and in most of them, a composite elongation below 10% was obtained. The most critical issue for these types of Al–Si alloys is the brittle plate-like eutectic silicon that causes failure during tensile loading even if an ideal dispersion of nanoparticles can be obtained. In fact, for the reinforcing of such alloys by NPs, eutectic silicon fragmentation into fine particles (or modification of eutectic silicon phase) is required in parallel to NPs addition.

Table 1
Mechanical properties reported for A356 composites in the literature.

Materials	Reinforcement Size and Type	Manufacturing Method	YS (MPa)	UTS (MPa)	Break Strain %	Remarks	Ref
			Before/ after HT	Before/ after HT	Before/ after HT		
A356-1 wt % SiC	Multi-sized particles	SS-SC followed by hot extrusion	131/-	228/-	8.5/-	Metallic carrier was used for a better wettability	[26]
A356-1 wt % SiC	40 nm, nanoparticles	SS-Squeeze casting followed by Ultrasonic assistant	–	181/-	2.7/-	After ultrasonic: UTS = 269 Break Strain = 6.2 Using Al powders as a modifier	[27]
A356-2 wt % SiC	40 nm, nanoparticles	LS-SC followed by Ultrasonic assistant and T6	144/-	259/-	5.3/-	Using Al powders as a modifier	[28]
A356-3 wt% ZrB_2+0.05 wt%Er	10–80 nm, nanoparticles	LS-electromagnetic stirring	250/-	325/-	13.65/-	Using in situ method	[29]
A356–0.9 wt % CNFs	Diameter of 50–200 nm, and length of 3–12 μm, nanowires	LS-ultrasonic vibration followed by extrusion	202/-	261/-	5/-	–	[30]
A356–0.5 wt% MWCNT	Outside ϕ 20–40 nm, inside ϕ 5–10 nm and length 10–30 nm, nanotubes	LS-SC followed by T6	–	-/277	–	–	[31]
A356–1.5 wt% MWCNT	Diameter of 10–100 nm, carbon nanotubes	SS- squeeze casting	157.7	245	6.93	–	[32]
A356-3 wt% ZrO_2	30 nm, nanoparticles	SS-SC followed by T6	–	165	4.7	–	[33]
Al356-1 vol% SiCp	50–56 μm, particles	LS-SC with Ultrasonic assistant followed by T6	-/183	-/257	-/7.5	Using hybrid stirring	[34]
Al356/5 vol% SiCp	10 μm, particles	LS-SC	120/-	160/-	4/-	Using Al powders as a modifier	[35]
A356/1.5 vol% Al_2O_3	20 nm, nanoparticles	LS-SC	230/-	265/-	1.12/-	Using Al powders as a modifier	[36]
A356/1.5 vol% nano – TiB_2	20 nm, nanoparticles	LS-SC	277/-	364.9/-	2.6/-	Using Al powders as a modifier	[37]
A356/1.5 vol% Al_2O_3	20 nm, nanoparticles	LS-SC	115/-	182/-	2.2/-	Using Al powders as a modifier	[14]
A356–1 wt% SiC	35 nm, nanoparticles	LS-SC	137/-	173/-	5.38/-	Using Al powders as a modifier	[38]
A356-5 wt-% of Ni-coated Al_2O_3	50 nm, nanoparticles	LS-SC	135.42/-	186.36/-	1.27/-	Electroless deposition Coating on nanoparticles	[39]
A356-2 wt% of Al_2O_3-10% ZrO_2	80 nm, nanoparticles	LS-SC	–	160/-	1/-	–	[40]
A356-5 wt-% Al_2O_3	60 nm, nanoparticles	SS-SC followed by squeeze casting	245/-	282/-	8/-	–	[41]
A356-0.1 wt% TiC	70–80 nm	LS-SC followed by T6	181/197	267/284	6.8/8.3	Using T6 heat treatment to modify alloy	[42]
A356–15 wt% SiC	25 μm, particles	Electromagnetic LS-SC	–	309.83/-	13.5/-	–	[43]
A356–2 wt% Al_2O_3	40 nm, nanoparticles	SS-SC	–	195/-	6.8/-	–	[44]
A356-2 wt-% SiC	≤30 nm, nanoparticles	Ultrasonic assisted LS-SC	150/-	300/-	4/-	–	[5]
A356–5 vol% SiCp	4 μm, particles	LS-SC followed by Rheo-process	–	268/-	5.2/-	Using a twin-screw machine to apply sufficient shear stress on particle clusters	[45]
A356–1 vol% SiC	40 nm, nanoparticles	SS-SC followed by Hot-rolling	196/-	292/-	12.4/-	Titanium was used as a modifier	[46]
A356–5 vol% SiCp	80 nm, nanoparticles	LS-SC	–	190/-	4.5/-	Aluminium was used as a modifier	[47]
A356–2 vol% SiCp	40 nm, nanoparticles	Ultrasonic assisted LS-SC followed by squeeze cast	–	226/-	5.5/-	Aluminium was used as a modifier	[48]
A356–3 wt% B_4C	100–300 nm, nanoparticles	LS-SC followed by Hot-extrusion	–	320/-	–	Aluminium was used as a modifier	[49]
A356–8.37 vol% TiB_2	In-situ particles	LS-SC followed by T6	217/347	258/391	2.73/ 1.32	In-situ method	[50]
A356-15 wt% SiC-5 wt% Fly-ash	25 μm, particles	Electromagnetic LS-SC followed by heat treatment	–	320/364	-/12	Using heat treatment to modify alloy	[51]
A356, 1.5 wt% alumina and 1.5 wt % SiC	Al_2O_3 170 μm, SiC 15 μm	SS-SC followed by Hot-rolling	237/-	302/-	5.2/-	Using Cu coted reinforcement by electroless deposition	[52]
A356, 1.5 wt% MWCNTs	10 nm in diameter,and10 μm in length carbon nanotubes	SS-SC followed by squeeze casting	150/-	250/-	7/-	Aluminium was used as a modifier	[53]
A356–10%B_4C	65 μm, particles	LS-SC followed by T6	160/200	180/280	0.7/0.5	Using heat treatment to modify alloy	[54]
A356-5 vol.% $ZrSiO_4$	<10 μm, particles	LS-SC	–	221/-	2.6/-	–	[55]
A356 -9 wt% SiC, 3 wt % Gr	1- 2 μm, particles	LS-SC	–	140/-	0.21/-	(C_2Cl_6) tablets were added, which decompose to form ($AlCl_3$) gas bubbles.	[56]
A356/10 vol% SiC	<5 μm, particles	SS-SC followed by ARB	–	348/-	6/-	–	[57]
A356–1.5 wt % Al_2O_3 and 1.5 wt % SiC	Al_2O_3 170 μm,SiC 15 μm Particles	SS-SC followed by Hot- rolling	253/-	325/-	5.4/-	Ni-coated Alumina and Cu-coated SiC For a better wettability	[58]

Table 2
Characteristics of the samples fabricated in this study.

Matrix	Reinforcement	Ball milling Time (h)	Ball milling Speed (rpm)	Ball to powder weight ratio	Semi-Solid Stirring Time (min)	Semi-Solid Stirring Tem (°C)	Liquid-state Stirring Time (min)	Liquid-state Stirring Tem (°C)	Hot-Rolling Tem (°C)
A356 (480±5g)	Ti (15g)-SiC_{np} (5g)	24	220	8:1	6	600	2	680	500
A356 (480±5g)	Ni (15g)-SiC_{np} (5g)	24	220	8:1	6	600	2	680	500

In this study, A356 based nanocomposites were prepared by solid-state modification of NPs using nickel and titanium as modifiers of the NPs, then stir casting process in two steps, followed by hot rolling (HR) to study the dispersion of β-SiC NPs within the matrix and associated physical effects.

2. Experimental procedures

2.1. Preparation of reinforcing phase

The reinforcement for the fabrication of the A356-based MMNCs was 1 wt% SiC NPs with an average particle size of 50 nm obtained from US-Research NanoMaterial Co. The benefit of the selection of SiC NPs is their higher thermal conductivity and modulus compared to Al_2O_3 NPs, for example. Besides, the relative density of SiC is closer to that of aluminium compared with alumina. Nickel and titanium (Shanghai Dinghan Chemical Co., Ltd. China) as the modifier agents were used to improve the dispersion of nanoparticles in the A356 matrix. The reason for using them as the modifier for the deagglomeration of nanoparticles was reported elsewhere [26]. For this purpose, a Fritsch Pulverisette P5 planetary ball mill was used under high purity (99.99%) argon gas. Details of the ball-milling process are given in Table 2. In the semi-solid metal, a high viscosity fluid can mechanically trap composite powders, including NPs in which case mechanical mixing can improve the mixing of composite powders in the composite. It should be mentioned that the mechanical shearing used for solidification processing in traditional metal matrix composites (with microparticles) does not work for submicron and nanosized particles, as the shearing force generated by the mechanical stirring decays rapidly and become too weak to separate the nanoparticles. This is a primary reason why the solid-state modification of NPs before powder-injection to the melt was examined in this study.

2.2. Preparation of the bulk composite

Bulk MMNCs were manufactured using an injection of the prepared composite powders into molten A356 aluminum alloy under high purity (99.999%) argon gas atmosphere. A356 alloy contains around 7 wt% silicon that suppresses the potential chemical reaction between liquid aluminum and the SiC NPs, and it prevents the formation of Al_4C_3 (brittle compound) at the particle-matrix interface below 700 °C. After the entire alloy in the crucible was melted, it was cooled to 600 °C, corresponding to a 0.3 solid fraction, based on analysis with Thermo-calc software [52]. At 600 °C, severe oxidation and burning of NPs can be avoided. Then, 1 wt % Mg chips as a wetting agent, prepared by machining, were added and stirring of the semi-solid alloy (using a ceramic coated stainless-steel impeller) at 400 rpm was initiated, while pre-

heated powders (pre-heating was done at 350 °C for 120 min in argon atmosphere to remove the moisture and impurities) along with Mg chips were added to the uniformly formed vortex over a period of approximately 6 min to increase the incorporation rate of SiC NPs within the liquid aluminum alloy. Stirring was stopped after 6 min of stirring in semi-solid condition, and the melt temperature was increased to 680 °C with a heating rate of 25 °C/min. It was observed previously [26,59] that the semi-solid condition is not enough for the required interaction of Ti and Ni with the melt such that a suitable releasing of the NPs did not occur. Therefore, the melt was stirred at 680 °C for an extra 2 min after 6 min stirring at the semi-solid state for a higher

https://doi.org/10.1016/j.msea.2019.138639

release of the NPs. After the completion of the stir casting process, the bottom valve was opened, and the melt was guided to a mould at room temperature. The samples produced by two-step stir casting were then prepared for the HR process. Fig. 1 shows the schematic of the manufacturing process of bulk MMNCs, which was in this study.

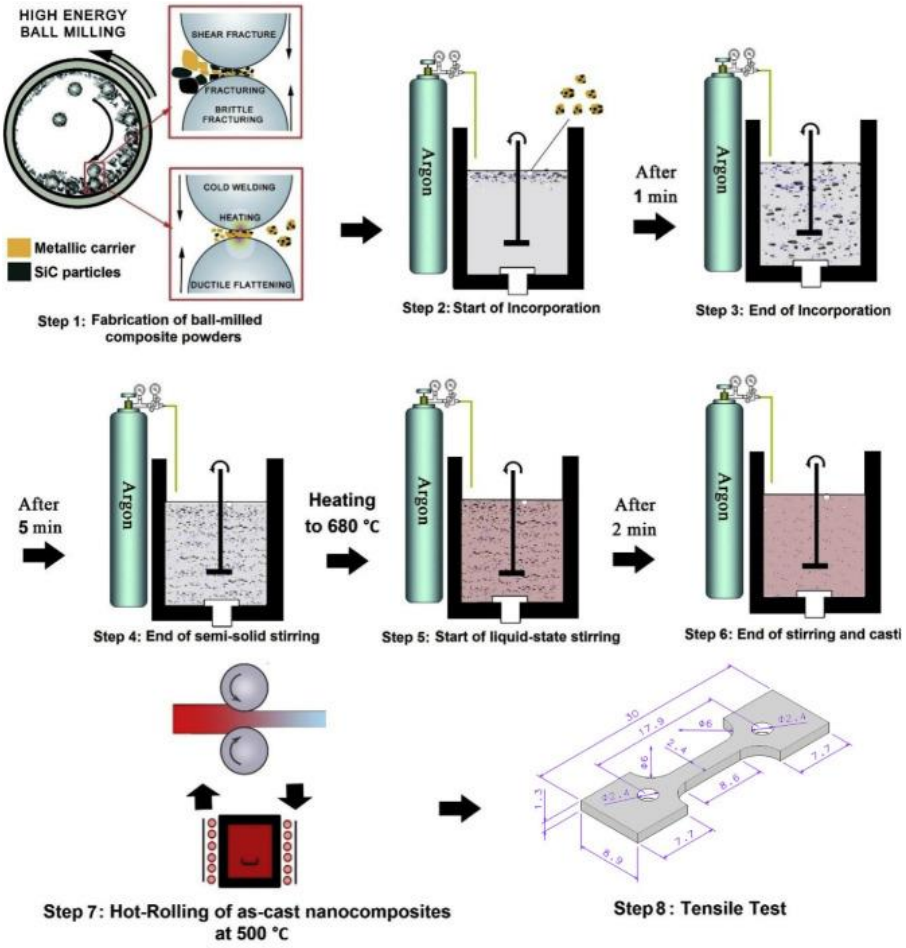

Fig. 1. Schematic of the manufacturing process implemented for this study.

2.3. Material characterization

Microstructure characterizations were performed using a field emission scanning electron microscope (FE-SEM, Mira 3, Tescan), operating at 10 kV and additionally equipped with an energy-dispersive X-ray spectrometer (EDS). For SEM study, the samples were ground, polished, and etched with Keller's reagent (190 ml water, 5 ml HNO_3, 3mlHCl, and 2 ml HF). Fractography was studied using a scanning electron microscope (SEM, Vega, Tescan, Electron Optic Services).

The phase composition, NP dispersion, and their interaction with dislocations were studied with a transmission electron microscope (TEM, JEM-2100, Jeol), operating at 200 kV. Samples for TEM analyses were prepared by site-specific Ga^+ focused ion beam milling process (FIB, 450S, FEI).

The tensile tests were performed at room temperature using a uniaxial tensile universal testing machine (Model 5982, Instron) of 100 kN operating capacity at a constant rate of crosshead displacement, with an initial strain rate of $2 \times 10{-}3\ s^{-1}$. For this purpose, plate tensile specimens with an 8.6 mm gauge length were prepared by the ASTM E8M standard and three

https://doi.org/10.1016/j.msea.2019.138639

repetitions. The YS (yield strength), UTS (ultimate tensile strength), and ductility (percent elongation to break) were measured.

3. Results and discussion

As described, solid-state modification of NPs using Ti and Ni metallic powders that effectively caused NPs breaking up due to repeated collisions between balls and powders and then semi-solid stirring at low temperature has some advantages as a suitable combined method for NPs dispersion within the melt. Fig. 2, Fig. 3 show the microstructure of nanocomposites containing Ti and Ni as the modifier agents, respectively, indicating that following liquid-state stirring after semi-solid stirring is a suitable complementary process that can complete gradual releasing of NPs. The formation of isolated, binary, and ternary SiC NPs after modification and their mechanical bonding with Ti and Ni without any reaction occurrence [26,59] could provide adequate wettability with the molten aluminium, and ensures their proper distribution by gradual releasing in the melt. Suitable dispersion of NPs within the grains with no observed segregation on grain boundaries can be observed (Fig. 2, Fig. 3a, b) for the two samples; additionally, no Ni segregation on the grain boundaries (Fig. 3c) was detected. Detection of many binary and ternary (or more) NPs in as-cast microstructure after their solid-state modification indicated that even intensive mechanical collisions of heavy balls cannot completely deagglomerate them, while it seems that using of a suitable metallic modifier followed by semi-solid and then liquid-state stirring can be an appropriate method for MMNCs manufacturing with uniform reinforcement distribution.

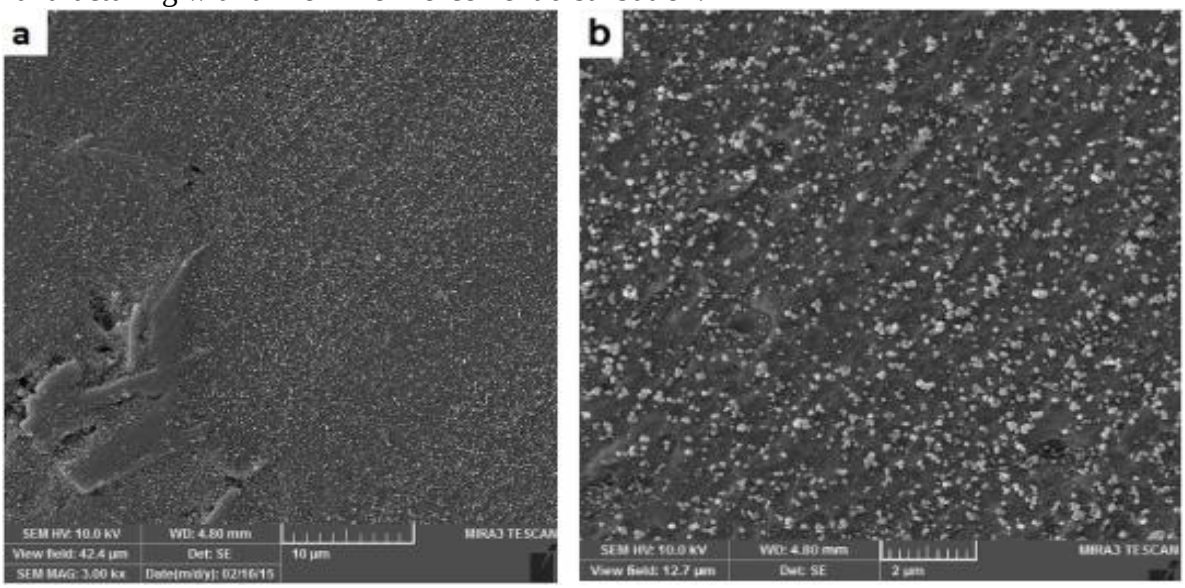

Fig. 2. SEM−SE micrograph of surface morphology of as cast samples for (a, b) Ti-1 wt. % SiC_{np}.

Manuscript version: 6 November 2019
Elsevier, Materials Science & Engineering
https://doi.org/10.1016/j.msea.2019.138639

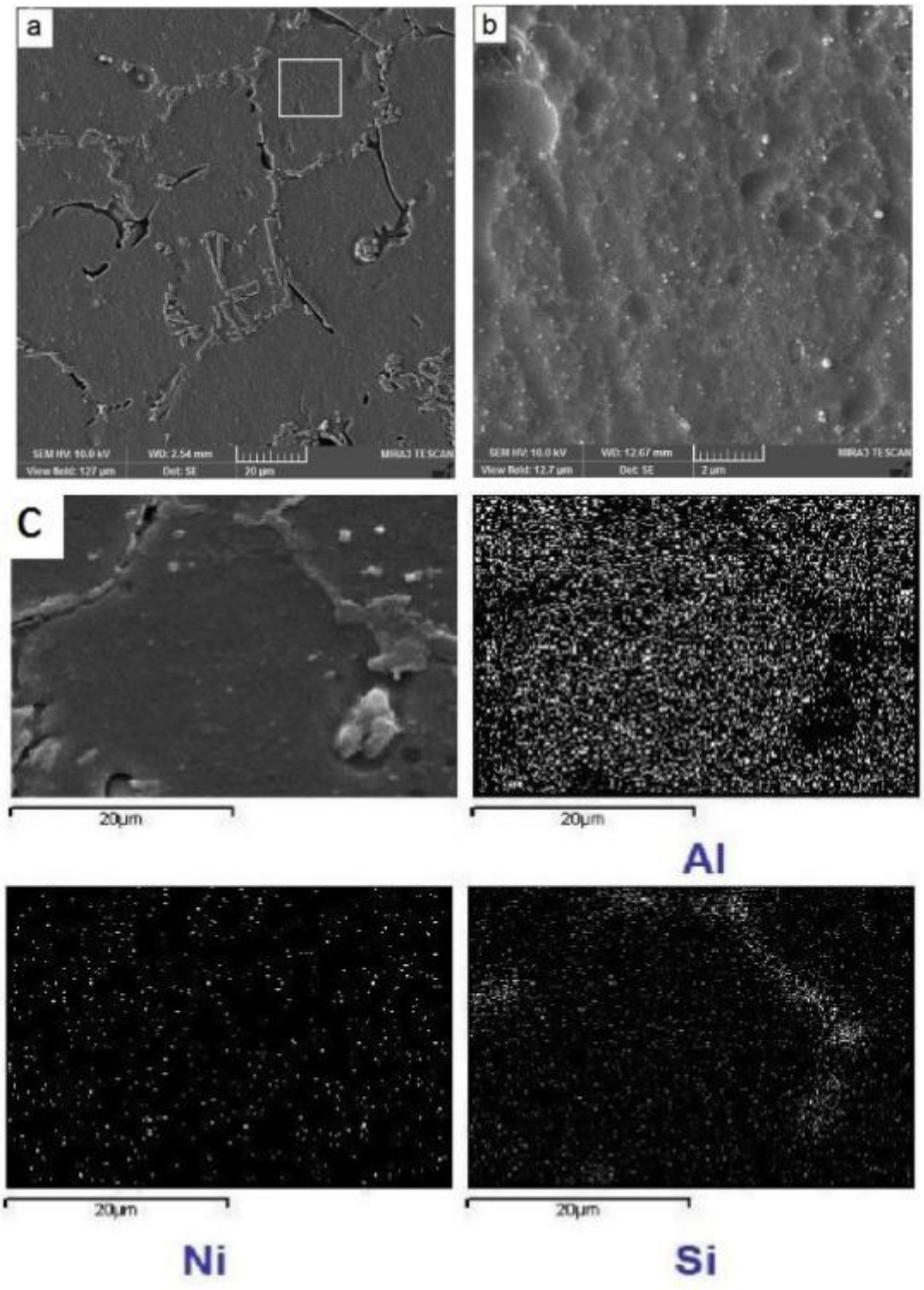

Fig. 3. SEM−SE micrograph of surface morphology of as cast samples for (a, b) Ni-1 wt. % SiC_{np}, (c) SEM−SE micrograph of surface morphology of as cast Ni-1 wt. % SiCnp, and corresponding EDS elemental mapping for Al, Ni and Si elements.

Fig. 4 shows a schematic of processes that occurred for the samples during stirring and solidification. It has been observed that the final microstructure of the developed A356 alloy consists of lamellar and flake-like Si plates embedded in the α-Al matrix without any tendency

https://doi.org/10.1016/j.msea.2019.138639

for segregation along the grain boundaries. Also, it can be observed that the interaction of Ti and Ni with aluminium melt (exothermic reaction) caused gradual releasing of NPs, resulting in their final engulfment and dispersion inside the grains.

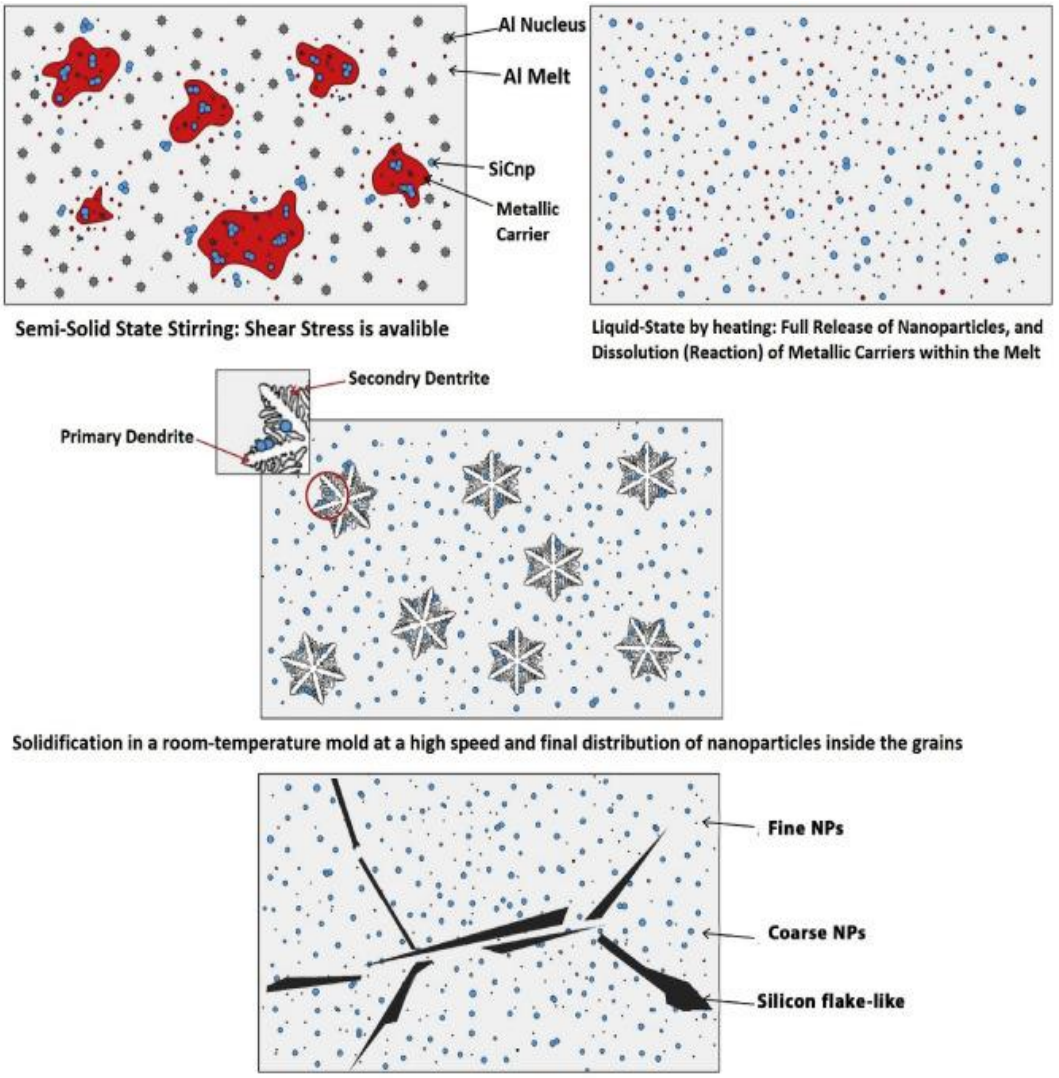

Fig. 4. Schematic of the microstructures obtained after solidification in this study.

Since Brownian motion can be considered as a mechanism that retards the movement of NPs, it seems that it will enhance the capture of NPs by the solidification front and improve their dispersion, therefore improving the chances of achieving Orowan strengthening. According to the Orowan mechanism, dislocation bowing is necessary for dislocations to bypass NPs. This motion of fine NPs can produce a considerable random movement that interrupts the settling behaviour of a particle and it has been reported that this motion will be considerable by decreasing the average size of NPs below 100 nm [25].

After casting, the HR process was applied to remove porosity, and related microstructure is shown in Fig. 2, Fig. 3a. Also, this process was applied to change the morphology and shape of flake-like eutectic silicon and make fine fragmented silicon particles. Fig. 5, Fig. 6 show SEM micrographs after the HR process, where we can observe how fine Si particles between 1 and 4 μm were obtained after the HR process. Also, a more suitable dispersion of fine and coarse NPs with a lower interparticle distance was obtained for the sample in which Ni was

https://doi.org/10.1016/j.msea.2019.138639

used as the modifier. To the best knowledge of authors, this suitable dispersion of NPs shown in Fig. 6a is among the best ones in aluminium matrix nanocomposites. It should be noted that the inter-particle distance of an ideal MMNCs reinforced by 1 wt % NPs should be considerably lower than as obtained in this study, indicating that the manufacturing of perfect distribution of nanoparticles in the MMNCs is complicated.

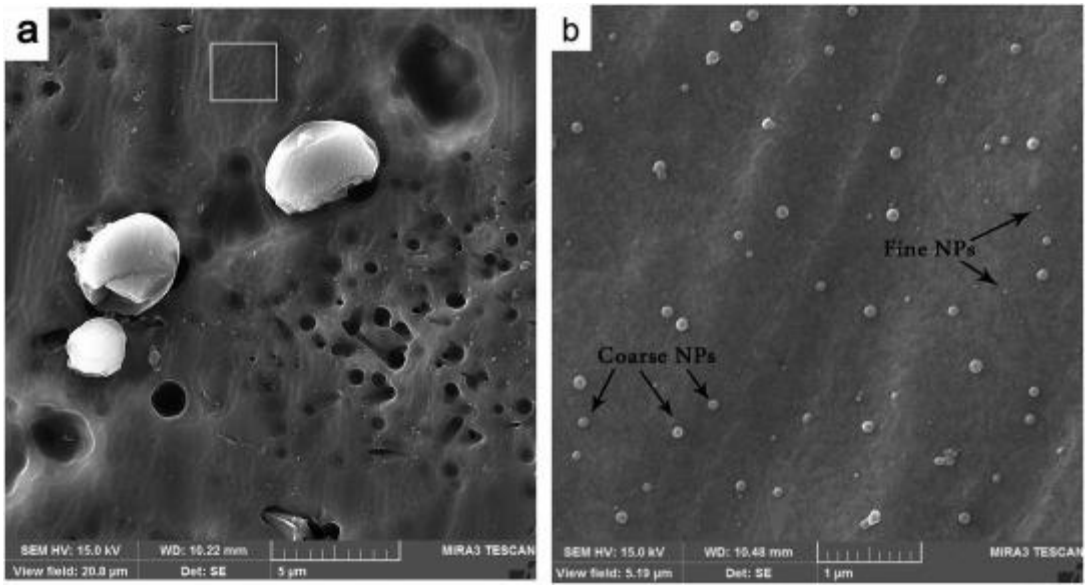

Fig. 5. SEM−SE micrograph of rolled Ti-1 Wt. % SiC_{np}, showing (a) remains of larger Si particles, and (b) fine and coarse NPs dispersion in matrix.

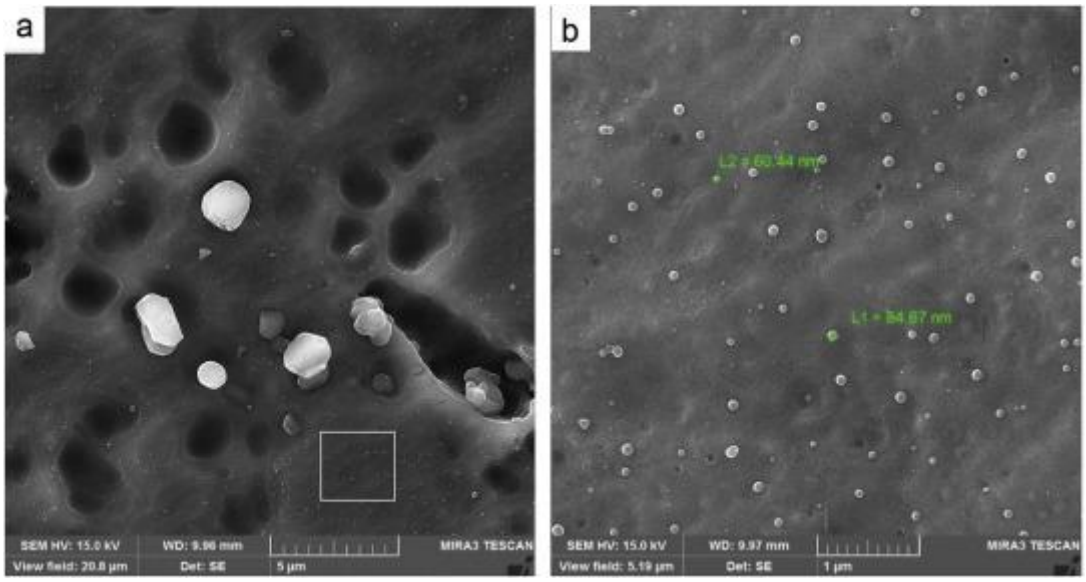

Fig. 6. SEM−SE micrograph of rolled Ni-1 wt. % SiC_{np} (a) low, (b) high magnification.

Fig. 7 shows electron-transparent FIB-produced lamella, containing Si fragments and almost an ideal dispersion of SiC NPs, without any agglomerates.

Manuscript version: 6 November 2019
Elsevier, Materials Science & Engineering
https://doi.org/10.1016/j.msea.2019.138639

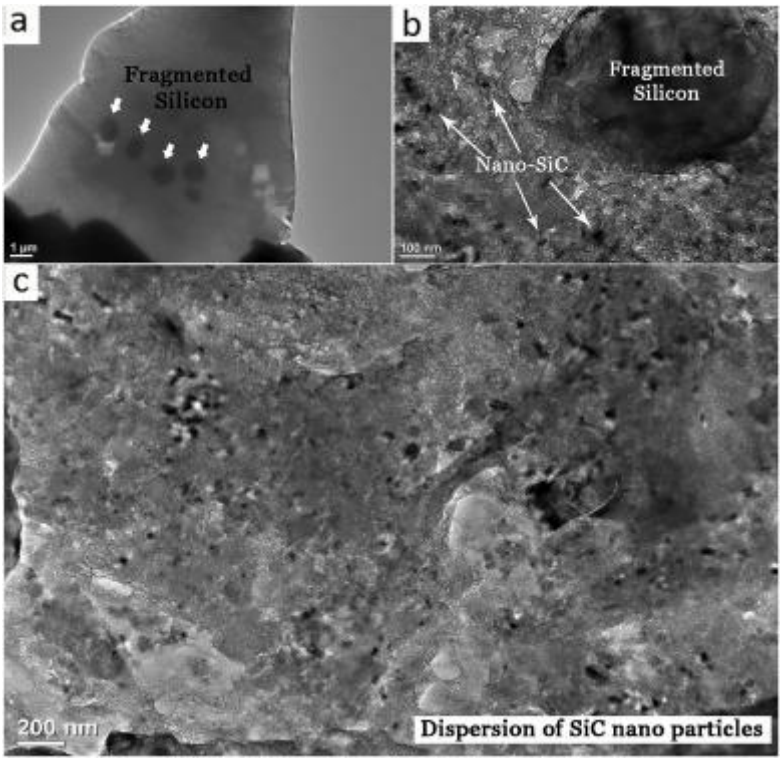

Fig. 7. Bright-field (BF) TEM micrographs of Ni-1 wt. % SiC_{np} microstructure, showing (a) overview TEM image of Si fragments in matrix, (b) dispersion of NPs around fragmented silicon particles, and (c) distribution and overall NPs dispersion in matrix.

The interaction between dislocations, controlling the mechanical properties of the investigated material, and the finely dispersed nanoparticles, are presented in Fig. 8, showing results obtained in three different areas. Several important conclusions can be drawn from these nanostructures: first, dislocation interact with NPs, and bowing mechanism occurred for fine SiC NPs, while no interaction of dislocations with coarse NPs was observed; Second, in some parts dislocation loops were observed; Third, the interaction of fine NPs with dislocation in this area was considerable. From Fig. 7 we can conclude that this investigated area is close to grain boundary as much silicon fragmentation was present. In this aspect, the NPs and dislocation interaction, combined with the bowing of dislocations, suggests that the presence of fine NPs can reduce and affect dislocation pile-up at grain boundaries. It should be mentioned that a negligible grain refinement was observed after casting of nanocomposites (see Supplementary Figs. S1, S2, and S3) and based on this interaction that was shown in Fig. 8, it can be deduced that the Orowan mechanism could be the main strengthening mechanism for the produced samples.

Manuscript version: 6 November 2019
Elsevier, Materials Science & Engineering
https://doi.org/10.1016/j.msea.2019.138639

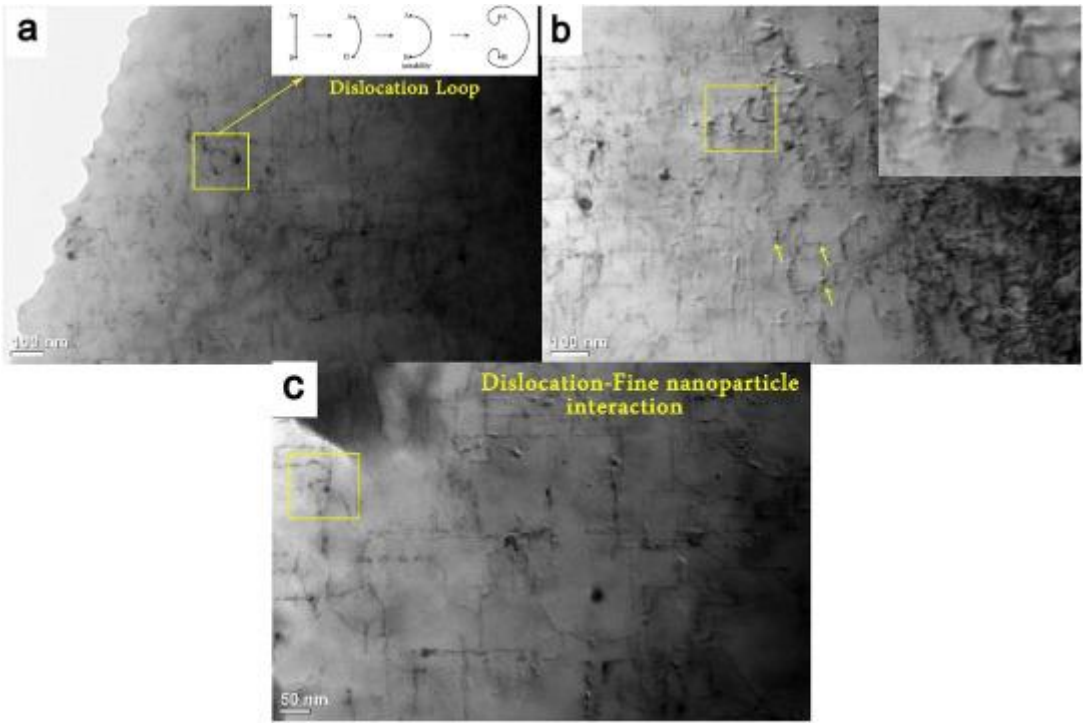

Fig. 8. BF-TEM micrograph of Ni-1 Wt. % SiC_{np} 2s sample showing interaction of dislocations with fine SiC NPs at various areas.

Based on the study by Xu et al. [60], more NP capture during solidification can occur when a core-shell nanoparticle, including a metallic core and ceramic shell face (SF). Following this report, some of the researchers in previous studies [59,61,62] tried to show the effect of metallic carriers (modifiers) on the Hamaker constant of ceramic NPs during solidification in aluminium matrix nanocomposites. Fig. 9 presents a TEM micrograph of an individual SiC NP embedded in an aluminium matrix as well as results of corresponding EDS analysis, excluding Ni presence around NP, suggesting core-shell structure after ball-milling might disappear during stirring and solidification due to a high interaction tendency of nickel and exothermic reaction with aluminium A356 melt at 680 °C [59]. Therefore, it seems that pure NPs facing the SF and Brownian motion might be the important reason for the capturing of NPs.

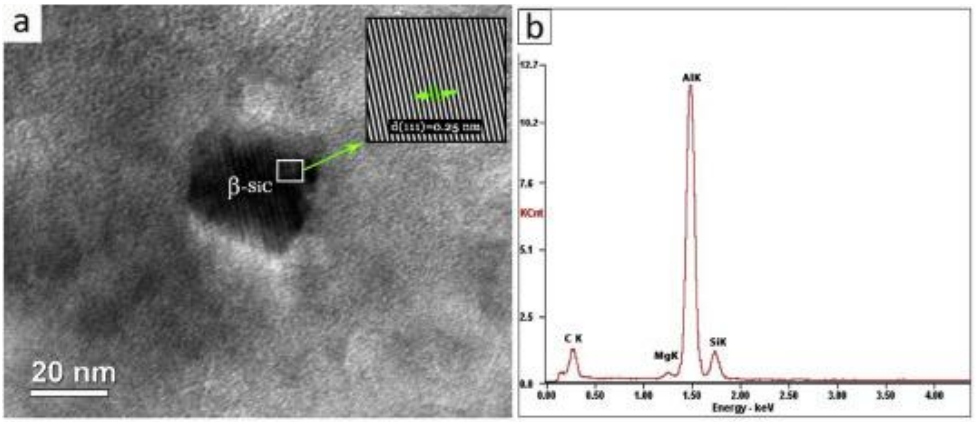

Fig. 9. a) TEM micrograph of a fine NP within aluminium matrix for Ni-1 Wt. % SiC_{np} 2s sample, identified as β-SiC, and (b) corresponding EDS spectra.

Manuscript version: 6 November 2019
Elsevier, Materials Science & Engineering
https://doi.org/10.1016/j.msea.2019.138639

As mentioned for Table 1, many researchers tried to improve the mechanical properties (strength-ductility trade-off) of A356 aluminium alloy. For this purpose, it was found that the morphology of eutectic silicon is the main prerequisite for strength-ductility trade-off. A comparison between microstructures of MMNCs after HR and before HR (compare Fig. 5, Fig. 6a with Fig. 2, Fig. 3a) show that the HR process as a severe plastic deformation technique completely fragmented the eutectic silicon phase into fine silicon particles and disperse them in the matrix. After this modification, the nano-scale reinforcing of the matrix based on the Orowan mechanism can be the second step for improving the mechanical properties. For this purpose, detachment of NPs from their initial condition and dispersing them in a matrix of Ni and Ti in solid-state was performed in this study. The gradual releasing of the NP from the Ni and Ti modifiers during stirring was discussed, and considerable interaction of fine NPs with dislocations was observed. Table 3, as well as Fig. 10, Fig. 11 summarize the tensile behavior of the reinforced and unreinforced samples and update of strength-ductility trade-off dilemma for A356 aluminum alloy. Unreinforced alloy after HR has a considerable combination of ductility and strength compared to many reported values in Table 1 due to fragmentation of eutectic silicon. After composite manufacturing, three changes occurred for A356 alloy. First, the addition of 1 wt % Mg as the wetting agent. Second, addition of 3 wt % Ni and Ti (separately), and third, suitable dispersion of SiC NPs inside the grains. Based on the literature [63,64], the addition of Mg, Ti, and Ni is not negligible on the strength of A356 alloy, especially after the T6 process. However, more than 77% and 70% increase in MMNCs for the UTS and elongation to failure, respectively, by using Ni as the modifier of NPs is emanated from well dispersion of NPs and their interaction with dislocations for avoiding dislocation pile-up, supporting Orowan strengthening mechanism. From Fig. 2, Fig. 5b, it can be deduced that the number of binary, ternary, and clusters of NPs in Ti-rich nanocomposite is higher than that of the other nanocomposite. It was reported in the literature [65] that at a temperature above 650 °C Ti, due to its tendency for oxidation, has a lower interaction with aluminum melt compared to Ni. Therefore, better performance of Ni as the modifier would be expected in the second step of stirring at liquid-state. It should be noted that some sparks were observed for Ni-rich samples during stirring at the second step of stirring at 680 °C. It is believed that more interaction of modifiers with the melt will lead to more heat release. Therefore, a higher amount of NPs releasing can occur, affecting the performance of the modifier. It was obtained that the Ti-rich sample had a considerable improvement in mechanical properties compared with the unreinforced sample, while its UTS and elongation to failure were lower than the Ni-rich samples.

Table 3
The mechanical properties of the samples after the rolling process.

Samples	UTS (MPa)	Break Strain (%)	YS (MPa)
Unreinforced A356	214^{+6}_{-4}	$9.6^{+0.1}_{-0.3}$	149^{+3}_{-3}
3 wt % Ti-1wt. % SiC_{np}	293^{+8}_{-9}	$12.8^{+0.7}_{-0.3}$	204^{+6}_{-7}
3 wt % Ni-1wt. % SiC_{np}	380^{+2}_{-7}	$16.4^{+0.1}_{-0.8}$	277^{+5}_{-3}

https://doi.org/10.1016/j.msea.2019.138639

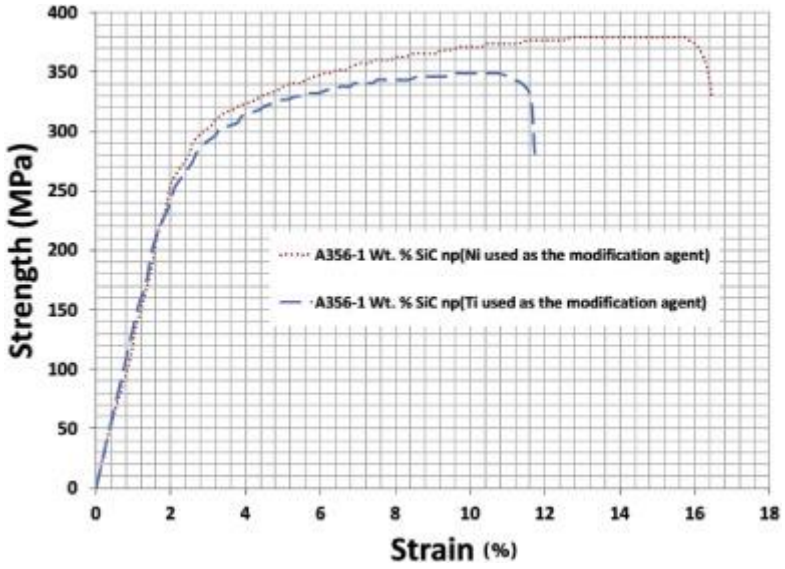

Fig. 10. Stress-strain curve of prepared samples after the HR process.

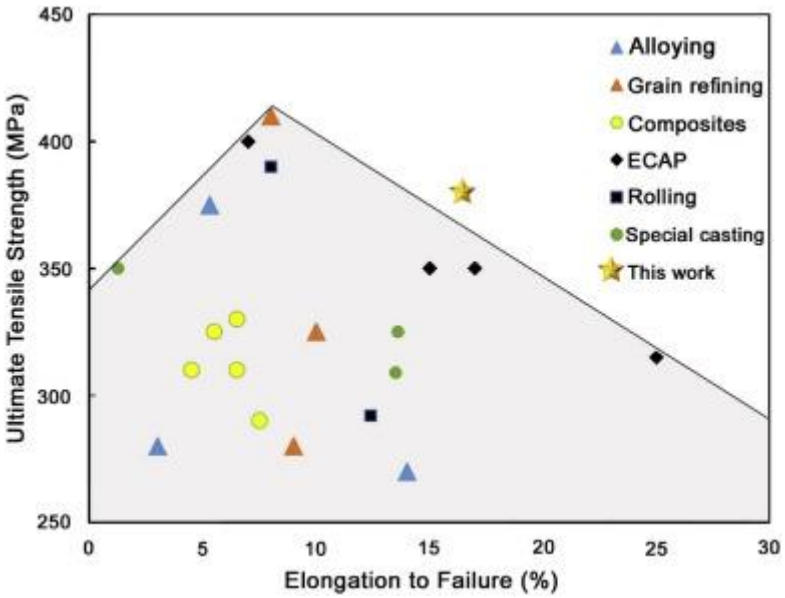

Fig. 11. Comparisons between the present tensile properties of A356 aluminium alloys fabricated using alloying, grain refining, composites, ECAP process [66], rolling process [46,66] and special casting process [29,43,66].

Very recently, researchers [66,67] reported strength-ductility trade-off for A356 aluminum alloy. Some impressive results were obtained in their study. Zhang et al. [65] used a complicated multi-step process, including four passes of equal channel angular pressing (ECAP) process with intermediate heat-treatment for the first step. Then after the T6 process, 80% cryo-rolling process was applied, and more than 480 MPa for UTS and 8.1% elongation to failure were obtained. Dang et al. [66] applied rapid solidification (96K/s) followed by post-heat treatment process and subsequent solid-solution treatment and quenching and finally, artificial aging for obtaining nano-sized eutectic silicon particles. More than 350 MPa for UTS and 21% elongation to failure were obtained after these steps, indicating the importance of Si

particle size and dispersion in the matrix. The interaction of dislocations with nano-sized silicon particles was shown in their study. However, Table 3 and Fig. 10 show that without any heat-treatment process, a considerable combination of UTS and elongation to failure was obtained in our study, indicating that if SiC NPs with a much higher Young modulus than Si is suitably dispersed in the matrix, then without any heat-treatment process, a trade-off of strength and ductility can be obtained. This is caused by the ceramic NPs acting as the barrier of dislocation movement. In fact, by simultaneous improvement of strength (by avoiding easy glide of dislocations), and ductility (by avoiding dislocation pile-up and stress accumulation at grain boundaries) the traditional concept of strength improvement that normally will lead to a reduction in elongation to failure will be overcome.

SEM micrographs of the fracture surface of the nanocomposite samples are presented in Fig. 12. More equiaxed dimples with a higher density were obtained for Ni-rich samples compared with Ti-rich nanocomposite. Moreover, smaller and shallower dimples were revealed for Ti-rich nanocomposite. Silicon and NP cluster debonding and fracture resulted in lower matrix deformation and formation of more small and shallow dimples.

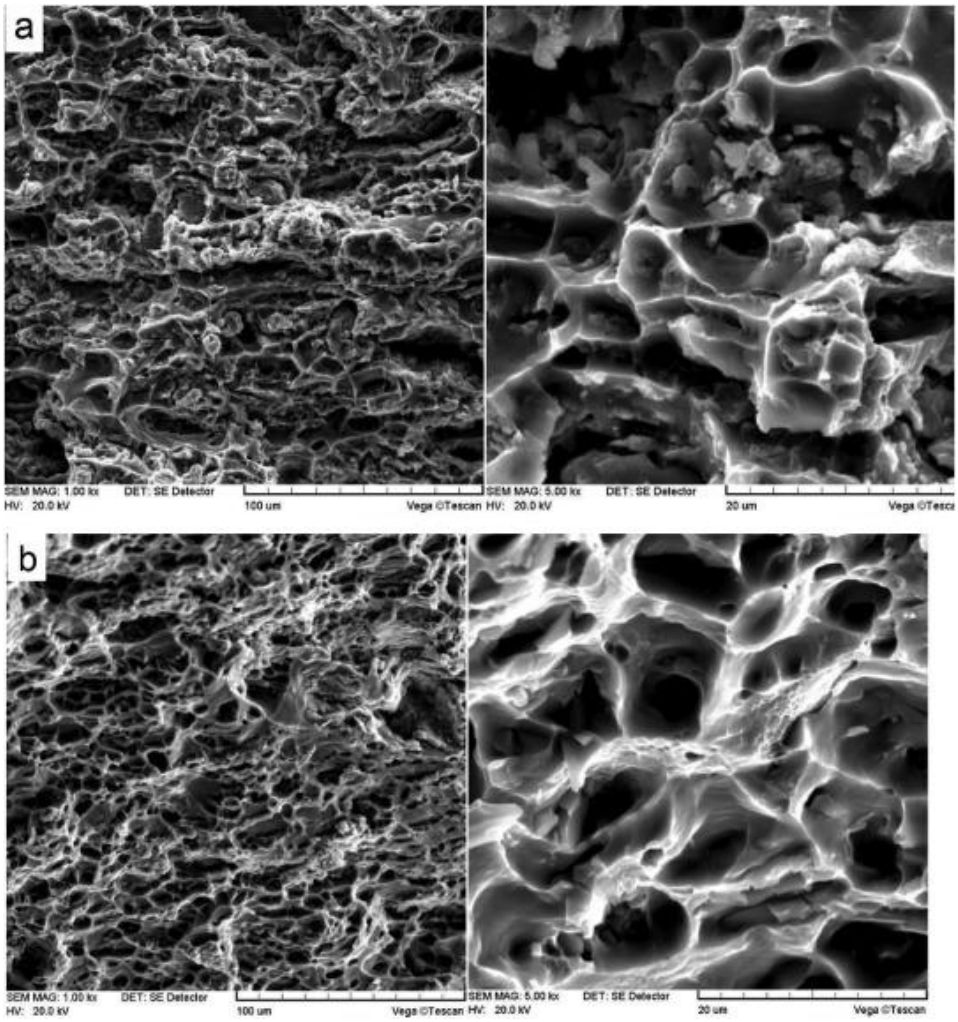

Fig. 12. The SEM−SE micrographs of the fracture surface of (a) Ti-1 Wt. % SiC_{np}, (b) Ni-1 Wt. % SiC_{np} samples.

In the future, we will optimize the ball-milling process for modification of NPs to reduce the number of binary and ternary NP clusters. Using a lower average size for NPs could likely lead to even higher interaction with dislocations, improving the mechanical properties even further.

4. Conclusions

In this study, solid-state modification of as-received NPs was implemented utilizing ball-milling with Ni and Ti as surface modifiers. The composite powders with a matrix of Ni and Ti (separately) were added to the semi-solid melt of A356 aluminium alloy. The stirring of the slurry was conducted in the semi-solid melt, followed by a stop for heating the slurry, and then in liquid-state stirring was continued. Finally, nanocomposite sheets were obtained by HR process. From the obtained results, the following conclusions can be drawn:

1. A suitable dispersion of fine and coarse NPs inside the grains was obtained after solidification and HR, especially for Ni-rich samples.

2. This suitable dispersion caused a considerable interaction of fine NPs with dislocations, and dislocation bowing was detected and shown.

3. With improved microstructure, a suitable combination of strength and ductility (380 MPa for UTS and 16.4% elongation to failure) was obtained for the Ni-rich samples compared to previous reports.

4. No Ni was detected around an individual fine SiC NP showing that Ni modifier interacted with melt during stirring, and they were not effective on the solidification process of NPs.

References

[1] J. Ferguson, G. Kaptay, B.F. Schultz, P.K. Rohatgi, K. Cho, C.-S. Kim

Brownian motion effects on particle pushing and engulfment during solidification in metal-matrix composites
Metall. Mater. Trans. A, 45 (2014), pp. 4635-4645

CrossRefView Record in ScopusGoogle Scholar

[2] I. El-Mahallawi, H. Abdelkader, L. Yousef, A. Amer, J. Mayer, A. Schwedt

Influence of Al 2 O 3 nano-dispersions on microstructure features and mechanical properties of cast and T6 heat-treated Al Si hypoeutectic alloys
Mater. Sci. Eng. A, 556 (2012), pp. 76-87

[3] X.-H. Chen, H. Yan

Solid–liquid interface dynamics during solidification of Al 7075–Al 2 O 3np based metal matrix composites
Mater. Des., 94 (2016), pp. 148-158

[4] S.O.R. Sheykholeslami, R.T. Mousavian, D. Brabazon

Corrosion behaviour of rolled A356 matrix composite reinforced with ceramic particles

Int. J. Mater. Res., 107 (2016), pp. 1100-1111

CrossRefView Record in ScopusGoogle Scholar

[5] Y. Yang, J. Lan, X. Li

Study on bulk aluminum matrix nano-composite fabricated by ultrasonic dispersion of nano-sized SiC particles in molten aluminum alloy
Mater. Sci. Eng. A, 380 (2004), pp. 378-383

ArticleDownload PDFView Record in ScopusGoogle Scholar

[6] L. Xiaochun, Y. Yang, D. Weiss

Theoretical and experimental study on ultrasonic dispersion of nanoparticles for strengthening cast Aluminum Alloy A356
Metall. Sci. Technol., 26 (2013)

Google Scholar

[7] S. Mula, P. Padhi, S. Panigrahi, S. Pabi, S. Ghosh

On structure and mechanical properties of ultrasonically cast Al–2% Al 2 O 3 nanocomposite
Mater. Res. Bull., 44 (2009), pp. 1154-1160

ArticleDownload PDFView Record in ScopusGoogle Scholar

[8]S. Donthamsetty

Investigations on mechanical properties of A356 nano composites reinforced with high energy ball milled SiC nanoparticles with ultrasonic assisted cavitation (with a comparison of micro composite)
Int. J. Nanoparticles (IJNP), 6 (2013), pp. 38-49

CrossRefView Record in ScopusGoogle Scholar

[9]H. Choi, M. Jones, H. Konishi, X. Li

Effect of combined addition of Cu and aluminum oxide nanoparticles on mechanical properties and microstructure of Al-7Si-0.3 Mg alloy
Metall. Mater. Trans. A, 43 (2012), pp. 738-746

CrossRefView Record in ScopusGoogle Scholar

[10]S. Kandemir, H.V. Atkinson, D.P. Weston, S.V. Hainsworth

Thixoforming of A356/SiC and A356/TiB2 nanocomposites fabricated by a combination of green compact nanoparticle incorporation and ultrasonic treatment of the melted compact
Metall. Mater. Trans. A, 45 (2014), pp. 5782-5798

CrossRefView Record in ScopusGoogle Scholar

[11]X.-H. Chen, H. Yan

Fabrication of nanosized Al 2 O 3 reinforced aluminum matrix composites by subtype multifrequency ultrasonic vibration
J. Mater. Res., 30 (2015), pp. 2197-2209

CrossRefView Record in ScopusGoogle Scholar

[12]L.-Y. Chen, J.-Q. Xu, H. Choi, M. Pozuelo, X. Ma, S. Bhowmick, *et al.*

Processing and properties of magnesium containing a dense uniform dispersion of nanoparticles

Nature, 528 (2015), p. 539

CrossRefView Record in ScopusGoogle Scholar

[13]H. Vishwanatha, J. Eravelly, C.S. Kumar, S. Ghosh

Microstructure and mechanical properties of aluminum-alumina bulk nanocomposite produced by a novel two-step ultrasonic casting technique
Metall. Mater. Trans. A, 47 (2016), pp. 5630-5640

CrossRefView Record in ScopusGoogle Scholar

[14]A. Mazahery, H. Abdizadeh, H. Baharvandi

Development of high-performance A356/nano-Al 2 O 3 composites
Mater. Sci. Eng. A, 518 (2009), pp. 61-64

ArticleDownload PDFView Record in ScopusGoogle Scholar

[15]K. Kumar, D. Verma, S. Kumar

Processing and tensile testing of 2024 Al matrix composite reinforced with Al2O3 nano-particles
5th International &26th All India Manufacturing Technology, Design and Research Conference, India (2014)

Google Scholar

[16]H. Ezatpour, M.T. Parizi, S.A. Sajjadi, G. Ebrahimi, A. Chaichi

Microstructure, mechanical analysis and optimal selection of 7075 aluminum alloy based composite reinforced with alumina nanoparticles
Mater. Chem. Phys., 178 (2016), pp. 119-127

ArticleDownload PDFView Record in ScopusGoogle Scholar

[17] H. Su, W. Gao, Z. Feng, Z. Lu

Processing, microstructure and tensile properties of nano-sized Al 2 O 3 particle reinforced aluminum matrix composites
Mater. Des., 36 (2012), pp. 590-596

1980-2015

ArticleDownload PDFView Record in ScopusGoogle Scholar

[18] L.-Y. Chen, J.-Y. Peng, J.-Q. Xu, H. Choi, X.-C. Li

Achieving uniform distribution and dispersion of a high percentage of nanoparticles in metal matrix nanocomposites by solidification processing
Scr. Mater., 69 (2013), pp. 634-637

ArticleDownload PDFView Record in ScopusGoogle Scholar

[19] J. Jiang, Y. Wang **Microstructure and mechanical properties of the semisolid slurries and rheoformed component of nano-sized SiC/7075 aluminum matrix composite prepared by ultrasonic-assisted semisolid stirring**

Mater. Sci. Eng. A, 639 (2015), pp. 350-358

ArticleDownload PDFView Record in ScopusGoogle Scholar

[20] L.-J. Zhang, F. Qiu, J.-G. Wang, Q.-C. Jiang

High strength and good ductility at elevated temperature of nano-SiC p/Al2014 composites fabricated by semi-solid stir casting combined with hot extrusion
Mater. Sci. Eng. A, 626 (2015), pp. 338-341

ArticleDownload PDFView Record in ScopusGoogle Scholar

[21]B. Schultz, J. Ferguson, P. Rohatgi

Microstructure and hardness of Al 2 O 3 nanoparticle reinforced Al–Mg composites fabricated by reactive wetting and stir mixing
Mater. Sci. Eng. A, 530 (2011), pp. 87-97

ArticleDownload PDFView Record in ScopusGoogle Scholar

[22]H. Su, W.L. Gao, H. Zhang, H.B. Liu, J. Lu, Z. Lu

Study on preparation of large sized nanoparticle reinforced aluminium matrix composite by solid–liquid mixed casting process
Mater. Sci. Technol., 28 (2012), pp. 178-183

CrossRefView Record in ScopusGoogle Scholar

[23] D.R. Kongshaug, J. Ferguson, B.F. Schultz, P.K. Rohatgi

Reactive stir mixing of Al–Mg/Al2O3np metal matrix nanocomposites: effects of Mg and reinforcement concentration and method of reinforcement incorporation
J. Mater. Sci., 49 (2014), pp. 2106-2116

CrossRefView Record in ScopusGoogle Scholar

[24]D. Zhou, F. Qiu, Q. Jiang

Simultaneously increasing the strength and ductility of nano-sized TiN particle reinforced Al–Cu matrix composites
Mater. Sci. Eng. A, 596 (2014), pp. 98-102

ArticleDownload PDFView Record in ScopusGoogle Scholar

[25]J. Ferguson, B.F. Schultz, P.K. Rohatgi, C.-S. Kim

Impact of Brownian motion on the particle settling in molten metals
Met. Mater. Int., 20 (2014), p. 747

CrossRefView Record in ScopusGoogle Scholar

[26]R.T. Mousavian, R.A. Khosroshahi, S. Yazdani, D. Brabazon, A. Boostani

Fabrication of aluminum matrix composites reinforced with nano-to micrometer-sized SiC particles
Mater. Des., 89 (2016), pp. 58-70

View Record in ScopusGoogle Scholar

[27]S. Lü, P. Xiao, D. Yuan, K. Hu, S. Wu

Preparation of Al matrix nanocomposites by diluting the composite granules containing nano-SiCp under ultrasonic vibaration
J. Mater. Sci. Technol., 34 (2018), pp. 1609-1617

ArticleDownload PDFView Record in ScopusGoogle Scholar

[28]K. Hu, D. Yuan, S.-l. LÜ, S.-s. Wu

Effects of nano-SiCp content on microstructure and mechanical properties of SiCp/A356 composites assisted with ultrasonic treatment
Trans. Nonferrous Metals Soc. China, 28 (2018), pp. 2173-2180

ArticleDownload PDFView Record in ScopusGoogle Scholar

[29]R. Tao, Y. Zhao, X. Kai, Y. Wang, W. Qian, Y. Yang, *et al.*

The effects of Er addition on the microstructure and properties of an in situ nano ZrB2-reinforced A356.2 composite

J. Alloy. Comp., 731 (2018), pp. 200-209

ArticleDownload PDFView Record in ScopusGoogle Scholar

[30]Q.-J. Wu, H. Yan

Fabrication of carbon nanofibers/A356 nanocomposites by high-intensity ultrasonic processing
Metall. Mater. Trans. A, 49 (2018), pp. 2363-2372

CrossRefView Record in ScopusGoogle Scholar

[31]H. Hanizam, M.S. Salleh, M.Z. Omar, A.B. Sulong

Optimisation of mechanical stir casting parameters for fabrication of carbon nanotubes–aluminium alloy composite through Taguchi method
J. Mater. Res. Technol., 8 (2) (2019), pp. 2223-2231

ArticleDownload PDFView Record in ScopusGoogle Scholar

[32]A.B. El Shalakany, B.M. Kamel, A. Khattab, T. Osman, B. Azzam, M. Zaki

Improved mechanical and tribological properties of A356 reinforced by MWCNTs
Fullerenes, Nanotub. Carbon Nanostruct., 26 (2018), pp. 185-194

CrossRefView Record in ScopusGoogle Scholar

[33]H. Tiwery, W. Hoziefa, B. Adel, I. El-Mahallawi

The effect of heat treatment on microstructure and mechanical properties of a356/zro2 nano reinforced composites
Proceedings of the 18th Int. AMME Conference (2018), p. 5

View Record in ScopusGoogle Scholar

[34]U. Aybarc, H. Yavuz, D. Dispinar, M.O. Seydibeyoglu

The use of stirring methods for the production of SiC-reinforced aluminum matrix composite and validation via simulation studies
Int. J. Metalcast., 13 (2019), pp. 190-200

CrossRefView Record in ScopusGoogle Scholar

[35]S. Amirkhanlou, B. Niroumand

Development of Al356/SiCp cast composites by injection of SiCp containing composite powders
Mater. Des., 32 (2011), pp. 1895-1902

ArticleDownload PDFView Record in ScopusGoogle Scholar

[36]M.K. Akbari, O. Mirzaee, H. Baharvandi

Fabrication and study on mechanical properties and fracture behavior of nanometric Al2O3 particle-reinforced A356 composites focusing on the parameters of vortex method
Mater. Des., 46 (2013), pp. 199-205

Google Scholar

[37]M.K. Akbari, H. Baharvandi, K. Shirvanimoghaddam

Tensile and fracture behavior of nano/micro TiB2 particle reinforced casting A356 aluminum alloy composites
Mater. Des., 66 (2015), pp. 150-161

1980-2015

View Record in ScopusGoogle Scholar

[38]Dehghan Hamedan, M. Shahmiri

Production of A356–1wt% SiC nanocomposite by the modified stir casting method
Mater. Sci. Eng. A, 556 (2012), pp. 921-926

ArticleDownload PDFView Record in ScopusGoogle Scholar

[39]

S. Pourhosseini, H. Beygi, S.A. Sajjadi

Effect of metal coating of reinforcements on the microstructure and mechanical properties of Al-Al2O3 nanocomposites
Mater. Sci. Technol. (2017), pp. 1-8

Google Scholar

[40]

M. Hajizamani, H. Baharvandi

Fabrication and studying the mechanical properties of A356 alloy reinforced with Al2O3-10% vol. ZrO2 nano-particles through stir casting
Adv. Mater. Phys. Chem., 1 (2011), p. 26

CrossRefView Record in ScopusGoogle Scholar

[41]

E.-S.Y. El-Kady, T.S. Mahmoud, M.A.-A. Sayed

Elevated temperatures tensile characteristics of cast A356/Al 2 O 3 nanocomposites fabricated using a combination of rheocasting and squeeze casting techniques
Mater. Sci. Appl., 2 (2011), p. 390

CrossRefGoogle Scholar

[42]

K. Borodianskiy, M. Zinigrad, A. Gedanken

Aluminum A356 reinforcement by carbide nanoparticles
J. Nano Res. (2011), pp. 41-46

View Record in ScopusGoogle Scholar

[43]

S.P. Dwivedi, S. Sharma, R.K. Mishra

Microstructure and mechanical properties of A356/SiC composites fabricated by electromagnetic stir casting
Procedia Mater. Sci., 6 (2014), pp. 1524-1532

ArticleDownload PDFView Record in ScopusGoogle Scholar

[44]

I. El-Mahallawi, Y. Shash, K. Eigenfeld, T. Mahmoud, R. Ragaie, A. Shash, *et al.*

Influence of nanodispersions on strength–ductility properties of semisolid cast A356 Al alloy

Mater. Sci. Technol., 26 (2010), pp. 1226-1231

CrossRefView Record in ScopusGoogle Scholar

[45]

S. Tzamtzis, N.S. Barekar, N. Hari Babu, J. Patel, B.K. Dhindaw, Z. Fan

Processing of advanced Al/SiC particulate metal matrix composites under intensive shearing – a novel Rheo-process
Compos. Appl. Sci. Manuf., 40 (2009), pp. 144-151

ArticleDownload PDFView Record in ScopusGoogle Scholar

[46]

S. Behnamfard, R.A. Khosroshahi, D. Brabazon, R.T. Mousavian

Study on the incorporation of ceramic nanoparticles into the semi-solid A356 melt
Mater. Chem. Phys., 230 (2019), pp. 25-36

ArticleDownload PDFView Record in ScopusGoogle Scholar

[47]

O. Yaghobizadeh, H.R. Baharvandi, A.R. Ahmadi, E. Aghaei

Development of the properties of Al/SiC nano-composite fabricated by stir cast method by means of coating SiC particles with Al
Silicon (2018), pp. 1-7

View Record in ScopusGoogle Scholar

[48]

S.-s. Wu, D. Yuan, S.-l. Lü, K. Hu, P. An

Nano-SiC P particles distribution and mechanical properties of Al-matrix composites prepared by stir casting and ultrasonic treatment
China Foundry, 15 (2018), pp. 203-209

CrossRefView Record in ScopusGoogle Scholar

[49]

M. Khademian, A. Alizadeh, A. Abdollahi

Fabrication and characterization of hot rolled and hot extruded boron carbide (B4C) reinforced A356 aluminum alloy matrix composites produced by stir casting method
Trans. Indian Inst. Met., 70 (2017), pp. 1635-1646

CrossRefView Record in ScopusGoogle Scholar

[50]

M. Wang, D. Chen, Z. Chen, Y. Wu, F. Wang, N. Ma, *et al.*

Mechanical properties of in-situ TiB2/A356 composites

Mater. Sci. Eng. A, 590 (2014), pp. 246-254

ArticleDownload PDFView Record in ScopusGoogle Scholar

[51]

S.P. Dwivedi, S. Sharma, R.K. Mishra

Microstructure and mechanical behavior of A356/SiC/Fly-ash hybrid composites produced by electromagnetic stir casting
J. Braz. Soc. Mech. Sci. Eng., 37 (2014), pp. 57-67

View Record in ScopusGoogle Scholar

[52]

N.B. Khosroshahi, R.T. Mousavian, R.A. Khosroshahi, D. Brabazon

Mechanical properties of rolled A356 based composites reinforced by Cu-coated bimodal ceramic particles
Mater. Des., 83 (2015), pp. 678-688

Google Scholar

[53]

A. B. Elshalakany, T. Osman, A. Khattab, B. Azzam, and M. Zaki, "Microstructure and mechanical properties of MWCNTs reinforced A356 aluminum alloys cast nanocomposites fabricated by using a combination of rheocasting and squeeze casting techniques," J. Nanomater., vol. 2014, 2014.

Google Scholar

[54]

H.R. Lashgari, S. Zangeneh, H. Shahmir, M. Saghafi, M. Emamy

Heat treatment effect on the microstructure, tensile properties and dry sliding wear behavior of A356–10%B4C cast composites
Mater. Des., 31 (2010), pp. 4414-4422

ArticleDownload PDFView Record in ScopusGoogle Scholar

[55]

K. Shirvanimoghaddam, H. Khayyam, H. Abdizadeh, M. Karbalaei Akbari, A.H. Pakseresht, F. Abdi, *et al.*

Effect of B4C, TiB2 and ZrSiO4 ceramic particles on mechanical properties of aluminium matrix composites: experimental investigation and predictive modelling

Ceram. Int., 42 (2016), pp. 6206-6220

ArticleDownload PDFView Record in ScopusGoogle Scholar

[56]

B. Viswanatha, M.P. Kumar, S. Basavarajappa, T. Kiran

Mechanical property evaluation of A356/SiCp/Gr metal matrix composites
J. Eng. Sci. Technol., 8 (2013), pp. 754-763

View Record in ScopusGoogle Scholar

[57]

R. Jamaati, S. Amirkhanlou, M.R. Toroghinejad, B. Niroumand

Comparison of the microstructure and mechanical properties of as-cast A356/SiC MMC processed by ARB and CAR methods
J. Mater. Eng. Perform., 21 (2011), pp. 1249-1253

Google Scholar

[58]

Y. Afkham, S. Fattahalhoseini, R.A. Khosroshahi, C. Avani, N. Mehrooz, R.T. Mousa vian

Incorporation of silicon carbide and alumina particles into the melt of A356 via electroless metallic coating followed by stir casting
Silicon, 10 (2018), pp. 2353-2359

CrossRefView Record in ScopusGoogle Scholar

[59]

R.T. Mousavian, R.A. Khosroshahi, S. Yazdani, D. Brabazon

Manufacturing of cast A356 matrix composite reinforced with nano-to micrometer-sized SiC particles
Rare Met., 36 (2017), pp. 46-54

CrossRefView Record in ScopusGoogle Scholar

[60]

J. Xu, L. Chen, H. Choi, X. Li

Theoretical study and pathways for nanoparticle capture during solidification of metal melt
J. Phys. Condens. Matter, 24 (2012), p. 255304

CrossRefView Record in ScopusGoogle Scholar

[61]

S. Behnamfard, R.T. Mousavian, R.A. Khosroshahi, D. Brabazon

A comparison between hot-rolling process and twin-screw rheo-extrusion process for fabrication of aluminum matrix nanocomposite
Mater. Sci. Eng. A, 760 (2019), pp. 152-157

ArticleDownload PDFView Record in ScopusGoogle Scholar

[62]

M.K. Akbari, K. Shirvanimoghaddam, Z. Hai, S. Zhuiykov, H. Khayyam

Al-TiB2 micro/nanocomposites: particle capture investigations, strengthening mechanisms and mathematical modelling of mechanical properties
Mater. Sci. Eng. A, 682 (2017), pp. 98-106

ArticleDownload PDFView Record in ScopusGoogle Scholar

[63]

D. Casari, T.H. Ludwig, M. Merlin, L. Arnberg, G.L. Garagnani

The effect of Ni and V trace elements on the mechanical properties of A356 aluminium foundry alloy in as-cast and T6 heat treated conditions
Mater. Sci. Eng. A, 610 (2014), pp. 414-426

ArticleDownload PDFView Record in ScopusGoogle Scholar

[64]

Z. Liu, X. Wang, Q. Han, J. Li

Effects of the addition of Ti powders on the microstructure and mechanical properties of A356 alloy
Powder Technol., 253 (2014), pp. 751-756

ArticleDownload PDFView Record in ScopusGoogle Scholar

[65]

M. Matsumuro, T. Kitsudo

Fabrication of in-situ intermetallic compound dispersed aluminum matrix composites by addition of metal powders
Mater. Trans., 47 (2006), pp. 2972-2979

CrossRefView Record in ScopusGoogle Scholar

[66]

X. Zhang, L. Huang, B. Zhang, Y. Chen, S. Duan, G. Liu, *et al.*

Enhanced strength and ductility of A356 alloy due to composite effect of near-rapid solidification and thermo-mechanical treatment

Mater. Sci. Eng. A, 753 (2019), pp. 168-178

[67]

B. Dang, X. Zhang, Y. Chen, C. Chen, H. Wang, F. Liu

Breaking through the strength-ductility trade-off dilemma in an Al-Si-based casting alloy
Sci. Rep., 6 (2016), p. 30874